Summary of Stress Analysis Results for the US-APWR Core Support Structures

Non-Proprietary Version

March 2009

Revision History

Revision	Page	Description
0	All	Original Issue

MITSUBISHI HEAVY INDUSTRIES, LTD.
16-5, Konan 2-chome, Minato-ku
Tokyo 108-8215 Japan

Abstract

This report contains a summary of the structural analysis of the six Core Support Structures parts prepared in accordance with MHI's commitment letter (Reference 6) concerning the content of this Technical Report.

The calculations were based on the loading conditions defined in the US-APWR Core Support Structure ASME Design Specification (Reference 4) and on the procedures per the ASME Boiler and Pressure Vessel Code Section III (Reference 1).

All of the stress intensity limits specified in the ASME Boiler and Pressure Vessel Code Section III Division 1 Subsection NG, 2001 Edition up to and including 2003 Addenda, are satisfied.

Table of Contents

List of Tables

List of Figures

List of Acronyms

The following list defines the acronyms used in this document.

CB	Core Barrel
CSS	Core Support Structures
CZF	Cold Zero Flow
DCD	Design Control Document
FEA	Finite Element Analysis
FSS	Full-power Steady State
FSRF	Fatigue Strength Reduction Factor
GT	Guide Tube
LBB	Leak-Before-Break
LCSP	Lower Corel Support Plate
LOCA	Loss-Of-Coolant Accident
NR	Neutron Reflector
NSS	No-power Steady State
RG	Regulatory Guide
RI	Reactor Internals
RCS	Reactor Coolant System
RSK	Radial Support Key
SCL	Stress Classification Lines
SCP	Stress Classification Planes
SRSS	Square Root of the Sum of the Squares
SSE	Safe Shutdown Earthquake
TSC	Top Slotted Column
TSF	Threaded Structural Fasteners
UCP	Upper Core Plate
UCS	Upper Core Support
USC	Upper Support Column

1.0 INTRODUCTION

This Technical Report summary of the stress analysis results for the US-APWR Core Support Structures (CSS) was prepared consistent with MHI's commitment letter (Reference 6) in support of the US-APWR DCD review process. The content of this report follows the ASME guidelines for Design Reports (Section III Division 1 Appendix C).

The CSS that constitutes the subassemblies of the reactor internals (RI) has a function to support the reactor core, which is defined in the CSS ASME Design Specification (Reference 4). Figure 1-1 shows a general configuration of the US-APWR RI.

The CSS are divided into the lower and upper CSS. The lower CSS consists of the Core Barrel (CB), the Lower Core Support Plate (LCSP), the Radial Support Keys (RSK), the LCSP Fuel Alignment Pins and Clevis Insert. The upper CSS consists of the Upper Core Support (UCS), the Upper Core Plate (UCP), the UCP Fuel Alignment Pins, the Upper Support Columns (USC), the Top Slotted Columns (TSC), the UCP Guide Pins and UCP Insert. Threaded Structural Fasteners (TSF) are included in both lower and upper CSS.

This report provides the structural evaluations for the six CSS parts based on discussion about MHI's commitment letter (Reference 6) the content of this Technical Report. The evaluated parts are tabulated in Table 1-1, and Figure 1-2 and Figure 1-3. This Technical Report summarizes the results and conclusions based upon detailed analyses that demonstrate the validity of the CSS components to meet the structural and thermal requirements of the CSS ASME Design Specification (Reference 4).

Table 1-1 Evaluated Parts of the CSS

No.	Evaluated Parts	Location of Evaluation	Ref.
1	Core Barrel (CB)	Flange / Upper CB discontinuity Upper CB / Lower CB discontinuity Lower CB / LCSP discontinuity	Figure 1-2
2	Lower Core Support Plate (LCSP)	All ligaments between core inlet holes	
3	Radial Support Key (RSK)	Root of the key body	
4	Upper Core Support (UCS)	All ligaments between holes for guide tube (GT) and USC Plate / skirt discontinuity Skirt / flange discontinuity	Figure 1-3
5	Upper Core Plate (UCP)	All ligaments between core outlet holes	
6	Upper Support Column (USC) including Top Slotted Column (TSC)	Column extensions Column bodies Column bottom fasteners	

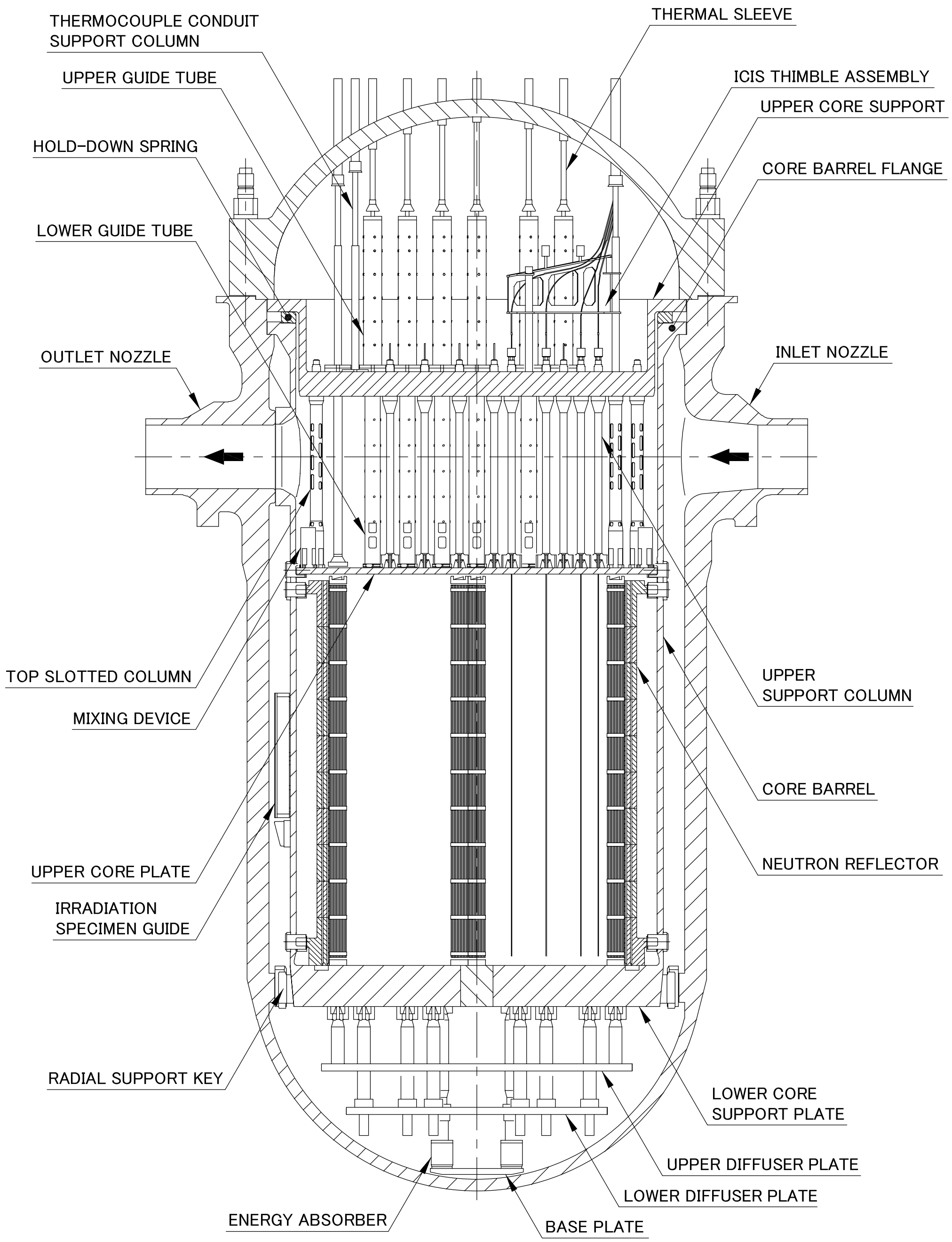

Figure 1-1 General Configuration of the US-APWR RI

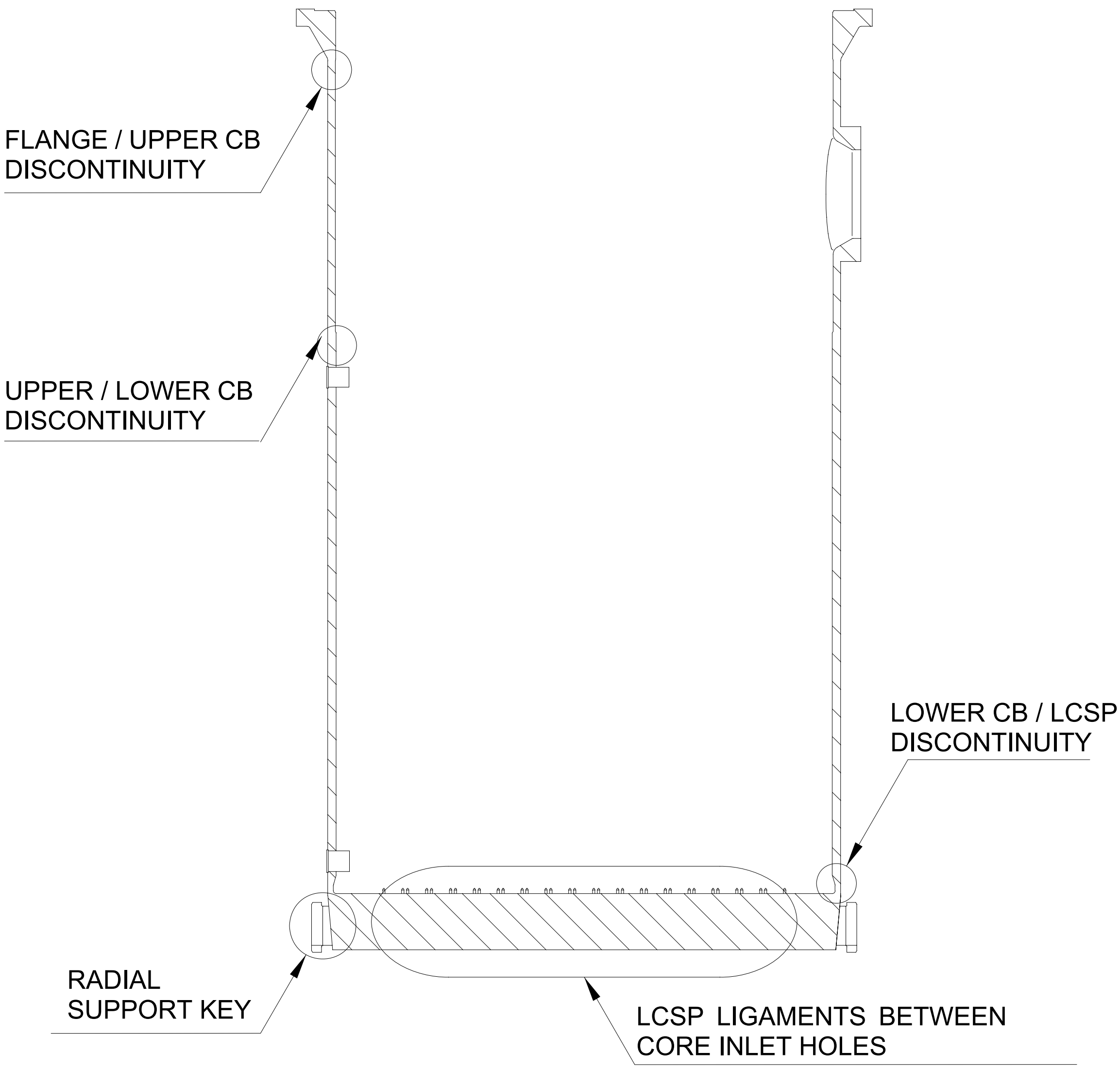

Figure 1-2 Stress Evaluation Points of the Lower CSS

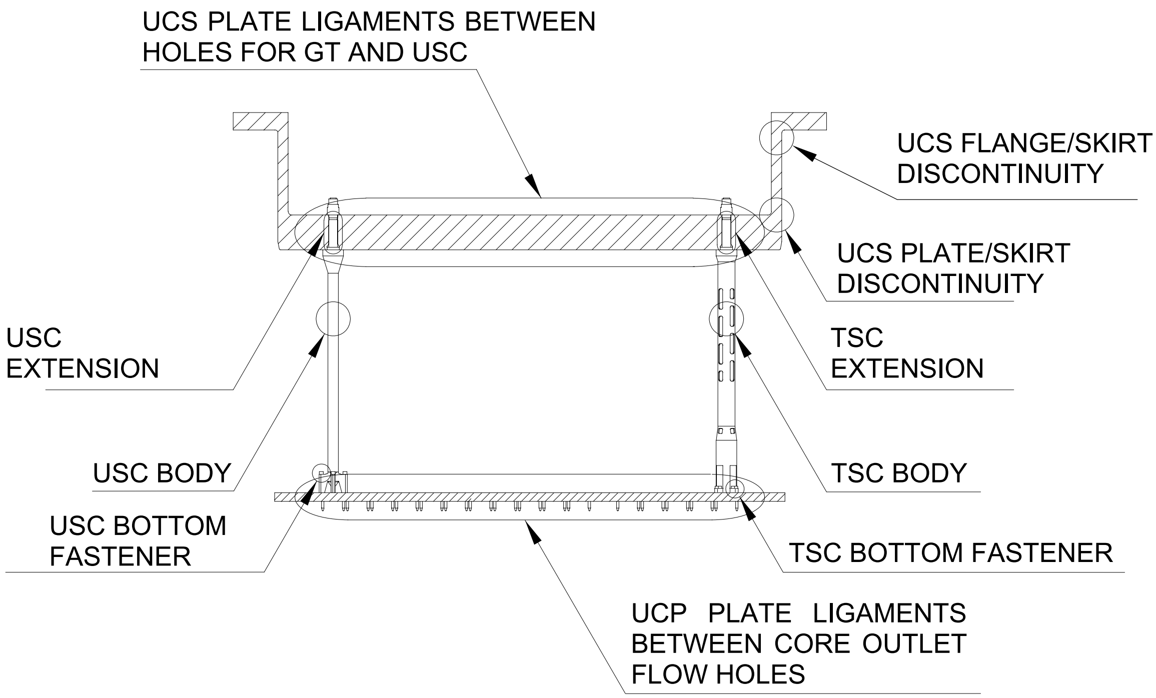

Figure 1-3 Stress Evaluation Points of the Upper CSS

2.0 SUMMARY OF RESULTS

The structural analysis results for each of the six parts evaluated, as mentioned in Section 1 are listed in Section 10. The most limiting results in each evaluation are listed in Table 2-1 below.

Table 2-1 Summary of Most Limiting Results

Section	Parts	Max Stress / Allowable Ratio[1)]	Highest Cumulative Fatigue Usage Factor, ΣU
10.1	Core Barrel		
	Lower Core Support Plate		
10.2	Upper Core Support		
	Upper Core Plate		
10.2 or 10.4	Upper Support Column [2)]		
10.3	Radial Support Key		

1) The allowable ratio is the "ratio" of the actual stress intensity to the allowable stress intensity.

$$\text{Ratio} = \frac{\text{Actual Stress Intensity}}{\text{Allowable Stress Intensity}}$$

2) Including the evaluation results for the TSC

3.0 CONCLUSIONS

The structural analysis for each of the six parts of the US-APWR CSS was performed in accordance with the ASME Boiler and Pressure Vessel Code, 2001 edition up to and including the 2003 Addenda for the Design and Service Conditions as specified in the CSS ASME Design Specification (Reference 4).

From the results summarized in this report, it is concluded that the six parts of the US-APWR CSS analyzed satisfy the ASME Code requirements for Design, Level A, Level B, Level C and Level D Service Conditions in the CSS ASME Design Specification (Reference 4).

4.0 NOMENCLATURE

Nomenclature used in this report is shown in Table 4-1

Table 4-1 Definitions of Nomenclature

Symbol	Unit	Definition
P_m	ksi	General Primary Membrane Stress
P_b	ksi	Primary Bending Stress
Q	ksi	Secondary Stress
Q_m	ksi	Secondary Membrane Stress
Q_b	ksi	Secondary Bending Stress
S_m	ksi	Design Stress Intensity
S_y	ksi	Yield Stress
S_u	ksi	Tensile Stress
σ_i	ksi	Primary Principal Stress Intensity (i =1,2,3)
1/3SSE	-	Level B Service Loading Earthquake
SSE	-	Safe Shutdown Earthquake

5.0 ASSUMPTIONS AND OPEN ITEMS

5.1 ASSUMPTIONS

The basic assumptions for the stress analysis are as follows:

1. All dimensions are taken from the nominal values in the CSS design drawings (Reference 7).

2. The CB finite element model does not include the outlet nozzles because;

    a. the outlet nozzle is not a CSS component,

    b. the outlet nozzle does not affect the structural integrity of the CB.

3. Although the components of the RI other than the CSS are not modeled, their weights are input into the CSS model as the external loads.

4. As for the RSK finite element model, chamfers in the key bottom and top, holes in the base plate, and cladding were not modeled since their effects on the stresses would be small, but the transition radii were modeled.

5.2 OPEN ITEMS

There are no open items in this Technical Report.

6.0 ACCEPTANCE CRITERIA

The stress intensity limits are taken from Subsubarticles NG-3220 and NG-3230 of the ASME Code, Section III (Reference 1). These limits are to be used in conjunction with loadings stated in Section 7.3. In order to evaluate the calculated stresses against these limits, it is necessary to classify or subdivide them. The NRC Regulatory Guide (RG) 1.207 guidance for the evaluation of environmental fatigue is separated from the ASME Design Requirement. This topic is beyond the scope of this report and will be evaluated separately.

6.1 STRESS LIMITS FOR OTHER THAN TSF

6.1.1 DESIGN LOADINGS (NG-3221)

Paragraph NG-3221 of the ASME Code (Reference 1) shows the stress intensity limits as below, which must be satisfied for the Design Loadings stated in the CSS ASME Design Specification (Reference 4). S_m is determined at Design Temperature (650°F) which is specified in the CSS ASME Design Specification (Reference 4).

(a) $P_m \leq S_m$

(b) $P_m + P_b \leq 1.5S_m$

(c) The external Design pressure difference shall not exceed the following allowable pressure difference P_a;

$$P_a = \frac{4B}{3D_0/T}$$

D_0 is the outside diameter of the CB and T is the minimum required thickness of the CB. B is determined by the material charts in Section II, part D, Subpart 3 of the ASME Code (Reference 3).

(d) The compressive stress of the USC and the TSC bodies shall not exceed the lesser of the S_m and B, which are described above.

6.1.2 Level A and Level B Service Limits (NG-3222 and NG-3223)

Paragraph NG-3222 of the ASME Code (Reference 1) shows the stress intensity limits for Level A and B Service Conditions as described below. S_m is determined at Service temperature.

(a) $P_m \leq S_m$

(b) $P_m + P_b \leq 1.5S_m$

(c) $P_m + P_b + Q \leq 3S_m$

For this exception, in lieu of meeting the $3S_m$ limit, an elastic-plastic fatigue analysis in accordance with Subparagraph NG-3228.3 of the ASME Code (Reference 1) shall be performed.

(d) For the fatigue analysis, the cumulative usage factor U specified in Subparagraph NG-3222.4 of the ASME Code (Reference 1) shall not exceed 1.0

(e) The evaluation of the thermal stress ratchet is in accordance with Subparagraph NG-3222.5 of the ASME Code (Reference 1). If a shakedown to an elastic condition occurs, this evaluation is not necessary to be performed.

6.1.3 Level C Service Limits (NG-3224)

Paragraph NG-3224 of the ASME Code (Reference 1) shows that the stress intensity limits for Level C Service Conditions are described below. S_m is determined at Service temperature.

(a) $P_m \leq 1.5S_m$

(b) $P_m + P_b \leq 2.25S_m$

6.1.4 Level D Service Limits (NG-3225)

Paragraph NG-3225 of the ASME Code (Reference 1) shows that the stress intensity limits for Level D Service Conditions are described below. S_m and S_u are determined at Service temperature. These expressions are described in Appendix F in Section III of the ASME Code (Reference 2).

(a) $P_m \leq$ the lesser of $2.4S_m$ and $0.7S_u$

(b) $P_m + P_b \leq$ the lesser of $3.6S_m$ and $1.05S_u$

6.1.5 Special Stress Limits (NG-3227)

Paragraph NG-3227 of the ASME Code (Reference 1) defines Special Stress Limits. For Level C and Level D Service limits are applied at 150% and 200% of Paragraph NG-3227 of the ASME Code (Reference 1), respectively. These stress intensity limits are not applied for the TSF.

(a) Bearing Loads

Paragraph NG-3227 of the ASME Code (Reference 1) shows that the average bearing loads must be limited to S_y at Design or Service temperature. This load is evaluated at the CB, UCS, and RSK.

(b) Triaxial Stresses

Paragraph NG-3227 of the ASME Code (Reference 1) shows that the algebraic sum of three primary principal stresses (σ_1+σ_2+ σ_3) does not exceed four times value of S_m as stated below.

$$\sigma_1 + \sigma_2 + \sigma_3 \leq 4S_m$$

6.2 STRESS LIMITS FOR TSF

6.2.1 DESIGN LOADINGS (NG-3231)

The stress limit for the primary membrane stress intensity defined in Subsubparagraph NG-3232.1(d) of the ASME Code (Reference 1) is applied as stated below. The Design stress intensity, S_m, is determined at Design Temperature.

$$P_m \leq S_m$$

6.2.2 LEVEL A AND LEVEL B SERVICE LIMITS (NG-3232 AND NG-3233)

Average Stress (NG-3232.1)

The limits for the average stress at Level A and Level B Service Conditions are described below. S_m, S_y and S_u are determined at Service temperature.

(a) $P_m + Q_m \leq$ the lesser of $0.9S_y$ and $\frac{2}{3}S_u$

(b) The average value of bearing stress under the fastener head shall be limited to $2.7S_y$.

(c) $P_m \leq S_m$

(d) The stress due to the preload shall be greater than that due to the primary and secondary membrane stress excluding the preload.

Maximum Stress (NG-3232.2)

The limits for the maximum stress at Level A and Level B Service Conditions are described below.

(a) $P_m + P_b + Q_m + Q_b \leq$ the lesser of $1.33 \times 0.9S_y$ and $1.33 \times \frac{2}{3}S_u$, where S_y and S_u are determined at Service temperature.

(b) The membrane stress intensity during installation of fasteners shall be no greater than the lesser of $1.2 \times 0.9S_y$ and $1.2 \times \frac{2}{3}S_u$, where S_y and S_u are determined at installation temperature.

<u>Fatigue Analysis (NG-3232.3)</u>

Cumulative usage factor shall not exceed 1.0, which is specified in Subparagraph NG-3232.3 of the ASME Code (Reference 1).

6.2.3 Level C Service Limits (NG-3234)

The stress intensity limits for Level C Service Conditions are described below. S_m is determined at Service temperature.

(a) $P_m \leq 1.5S_m$

(b) $P_m + P_b \leq 2.25S_m$

6.2.4 Level D Service Limits (NG-3235)

Level D Service limits are defined in accordance with Paragraph NG-3235 of the ASME Code (Reference 1) as below. S_m and S_u are determined at Service temperature. These expressions are described in Appendix F in Section III of the ASME Code (Reference 2).

(a) $P_m \leq$ the lesser of $2.4S_m$ and $0.7S_u$

(b) $P_m + P_b \leq$ the lesser of $3.6S_m$ and $1.05S_u$

7.0 DESIGN INPUT

7.1 GEOMETRY

The set of the drawings used to supply dimensions for the stress analysis is listed in Table 7-1. These drawings are included in the CSS Design Drawings (Reference 7).

Table 7-1 Drawing List

No.	Drawing Title	Drawing Number	Revision
1	Core Support Structures Design Drawings	N0-EC40101	0

7.2 MATERIAL

The materials for the CSS are listed in Table 7-2, which are specified in the CSS ASME Design Specification (Reference 4). The material and physical property data for each material were obtained from the ASME Code Section III Appendix I (fatigue properties) and Section II Part D (Reference 1 and 3). Tables 7-3 through 7-6 show the material strength properties used in the stress analyses and evaluations.

Table 7-2 Materials for the CSS

Part		Material
CB	Flange	ASME SA336 GR. F304
	Cylinder	ASME SA240 TYPE304
LCSP		ASME SA336 GR. F304
UCS	Flange	ASME SA336 GR. F304
	Skirt	ASME SA240 TYPE304
	Plate	ASME SA336 GR. F304
UCP		ASME SA240 TYPE304
USC	Body	ASME SA213 TYPE304
	Extension	ASME SA479 TYPE304
	Bottom Fastener	ASME SA479 TYPE316 Strain Hardened
TSC	Body	ASME SA312 TYPE304
	Extension	ASME SA479 TYPE304
	Bottom Fastener	ASME SA193 CLASS2 B8M
RSK		ASME SA182 GR. F304

Table 7-3 Material Properties for SA240, SA213, SA312 and SA479 TYPE304

Temperature [°F]	Sm [ksi]	Sy [ksi]	Su [ksi]
100	20.0	30.0	75.0
200	20.0	25.0	71.0
300	20.0	22.4	66.2
400	18.6	20.7	64.0
500	17.5	19.4	63.4
600	16.6	18.4	63.4
650	16.2	18.0	63.4

Table 7-4 Material Properties for SA336 and SA182 GR. F304

Temperature [°F]	Sm [ksi]	Sy [ksi]	Su [ksi]
100	20.0	30.0	70.0
200	20.0	25.0	66.3
300	20.0	22.4	61.8
400	18.6	20.7	59.7
500	17.5	19.4	59.2
600	16.6	18.4	59.2
650	16.2	18.0	59.2

Table 7-5 Material Properties for SA479 TYPE316 Strain Hardened

Temperature [°F]	Sm1) [ksi]	Sy1) [ksi]	Su1) [ksi]
100	28.3	65.0	85.0
200	28.3	59.8	85.0
300	26.8	56.5	80.3
400	25.9	54.0	77.6
500	25.7	52.3	77.1
600	25.7	51.4	77.1
650	25.7	50.9	77.1

1) These material property data were obtained from Reference 8.

Table 7-6 Material Properties for SA193 Class2 B8M

Temperature [°F]	Sm1) [ksi]	Sy1) [ksi]	Su1) [ksi]
100	31.6	65.0	90.0
200	31.6	59.8	90.0
300	29.9	56.5	85.1
400	29.0	54.0	82.4
500	28.7	52.3	81.6
600	28.7	51.4	81.6
650	28.7	50.9	81.6

1) These material property data were obtained from Reference 8.

7.3 LOADS, LOAD COMBINATIONS, AND TRANSIENTS

The loads, load combinations and transients are defined in the CSS ASME Design Specification (Reference 4). The following is a summary of those used for the CSS structural evaluations.

7.3.1 DESIGN PRESSURE DIFFERENCE AND DESIGN TEMPERATURE

Design Pressure Difference and Design Temperature are 87psi and 650°F, which are specified in the Design Specification (Reference 4), respectively.

7.3.2 MECHANICAL LOADS

The mechanical load is comprised of static load and dynamic load. The static load is given as pressure difference, dead weight, cross flow load, and interface load. The dead weight includes buoyancy load, and interface load consists of superimposed load, lift load, and dead weight of the components attached to the CSS. The cross flow load acts on USC and TSC. The dynamic load is given as vibratory load, 1/3SSE load, SSE+LOCA load. These loads are described in the CSS ASME Design Specification (Reference 4). The loads are summarized in Figure 7-1.

(1) Design Mechanical Loadings

Tables 7-7 through 7-12 summarize the Design Mechanical Loads.

(2) Level A and Level B Service Loadings

The loads for each Service Condition of the Cold Zero Flow (CZF), the No-power Steady State (NSS), and the Full-power Steady State (FSS) were defined in the CSS ASME Design Specification (Reference 4). The loads applied to the stress evaluations were selected depending on the thermal transients. The dynamic loads in Level A and Level B Service were substituted for the Design Mechanical Loads for conservatism. The static loads in Level A and Level B Service are shown in Tables 7-13 through 7-15

As for Level B Service loadings, the 1/3 SSE seismic loads shown in Tables 7-16 through 7-18 were taken into account. These loads were used only for the fatigue evaluations. The number of cycles is 300.

(3) Level C Service Loadings

For Level C Service Condition, only the primary stresses were evaluated. The Design Mechanical Loads were used for the evaluation at Level C Service because the mechanical loads at Level C Service are smaller than the Design Mechanical Loads, which are described in the CSS ASME Design Specification (Reference 4).

(4) Level D Service Loadings

For Level D Service Condition, only the primary stresses were evaluated. The loads used for the stress evaluations were the seismic and the accident loads. The SSE loads were applied for the seismic (earthquake) loads. The LOCA loads were applied for the accident “Large Loss of Coolant Accident” described in Table 7-23, which are based on the Leak-Before-Break (LBB) methodology. The SSE and LOCA loads were combined by “square root of the sum of the squares” (SRSS) method and are shown in Tables 7-19 through 7-21.

Table 7-7 Static Loads of the Lower CSS at Design Condition

Loading Source	Load
Pressure Difference of CB	
Dead Weight (in Water) Upper CB Lower CB LCSP	
Interface Load from Lower Diffuser Plate Assembly Upper Diffuser Plate Assembly Neutron Reflector Core Region Hold Down Spring	

Table 7-8 Static Loads of the Upper CSS at Design Condition

Loading Source	Load
Dead Weight (in Water) UCS USC TSC UCP	
Interface Load from Upper Internals Core Region Hold Down Spring	
Cross flow Load to USC Top of column Top of column body Bottom of column body Bottom of column TSC Top of column Top of column body Top of perforated cross section Bottom of small dia. region Bottom of column	

Table 7-9 Static Load of the RSK at Design Condition

Loading Source	Load
Installation Load	

Table 7-10 Dynamic Loads of the Lower CSS at Design Condition

Portion	Load		
	Axial [lbf]	Shear [lbf]	Moment [lbf-in]
LCSP			
CB Flange			
CB Middle Elevation			
CB Bottom End			

Table 7-11 Dynamic Loads of the Upper CSS at Design Condition

Portion	Load		
	Axial [lbf]	Shear [lbf]	Moment [lbf-in]
UCS Plate			
UCP			
UCS Skirt Top			
UCS Skirt Bottom			
USC			
Top of column			
Top of column body			
Bottom of column body			
Bottom of column			
TSC			
Top of column			
Top of column body			
Top of perforated cross section			
Bottom of small dia. region			
Bottom of column			

Table 7-12 Dynamic Load of the RSK at Design Condition

Portion	Load
Key (Bounding FIV Circumferential Force per Key)	

Table 7-13 Static Loads of the Lower CSS at Level A/B Service

Loading Source	Load		
	CZF	NSS	FSS
Pressure Difference of CB			
Dead Weight (in Water) Upper CB Lower CB LCSP			
Interface Load from Lower Diffuser Plate Assembly Upper Diffuser Plate Assembly Neutron Reflector Core Region Hold Down Spring			

Table 7-14 Static Loads of the Upper CSS at Level A/B Service

Loading Source	Load		
	CZF	NSS	FSS
Dead Weight (in Water) UCS USC TSC UCP			
Interface Load from Upper Internals[2)] Core Region Hold Down Spring			
Cross flow Load to USC Top of column Top of column body Bottom of column body Bottom of column TSC Top of column Top of column body Top of perforated region Bottom of small dia. region Bottom of column			

2) This value includes the hydraulic force on the UCS.

Table 7-15 Static Loads of the RSK at Level A/B Service

Loading Source per Key	Bounding Load		
	CZF [lbf]	NSS [lbf]	FSS [lbf]
Interface load (Circumferential-Direction)			
Friction load due to thermal expansion (Radial-Direction)			
Friction load due to thermal expansion (Axial-Direction)			

Table 7-16 1/3SSE LoadsApplied to the Lower CSS

Portion	Load Axial [lbf]	Load Shear [lbf]	Load Moment [lbf-in]
LCSP			
CB Flange			
CB Middle Elevation			
CB Bottom End			

Table 7-17 1/3 SSE Loads Applied to the Upper CSS

Portion	Load Axial [lbf]	Load Shear [lbf]	Load Moment [lbf-in]
UCS Plate			
UCP			
UCS Skirt Top			
UCS Skirt Bottom			
USC			
Top of column			
Top of column body			
Bottom of column body			
Bottom of column			
TSC			
Top of column			
Top of column body			
Top of perforated cross section			
Bottom of small dia. region			
Bottom of column			

Table 7-18 1/3 SSE Bounding Load Applied to the RSK

Portion	Load
Key (Circumferential Force per Key)	

Table 7-19 SSE+LOCA Loads Applied to the Lower CSS

Portion	Load Axial [lbf]	 Shear [lbf]	 Moment [lbf-in]
LCSP			
CB Flange			
CB Middle Elevation			
CB Bottom End			

Table 7-20 SSE+LOCA Loads Applied to the Upper CSS

Portion	Load Axial [lbf]	 Shear [lbf]	 Moment [lbf-in]
UCS Plate			
UCP			
UCS Skirt Top			
UCS Skirt Bottom			
USC			
Top of column			
Top of column body			
Bottom of column body			
Bottom of column			
TSC			
Top of column			
Top of column body			
Top of perforated cross section			
Bottom of small dia. region			
Bottom of column			

Table 7-21 SSE+LOCA Bounding Loads Applied to the RSK

Portion	Load
Key (Circumferential Force per Key)	

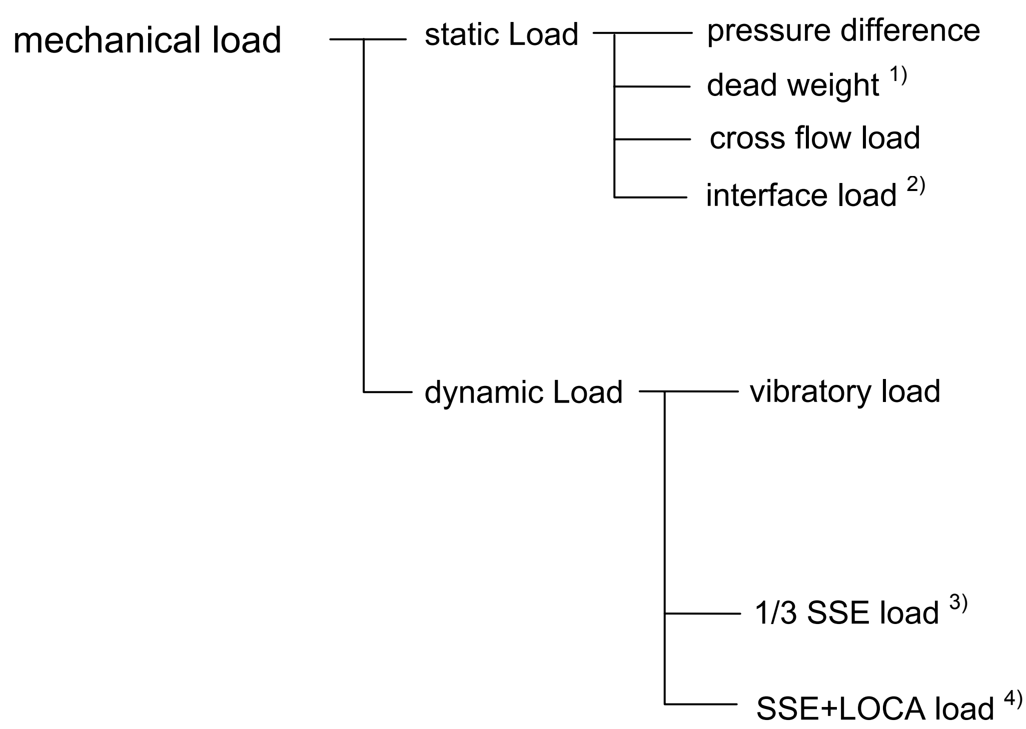

Note

1) The dead weight includes the buoyancy load.

2) The interface load consists of the superimposed load, lift load, and dead weight of the components other than the CSS.

3) The 1/3 SSE load is only applied to Level B Service Condition.

4) The SSE+LOCA load is only applied to Level D Service Condition.

Figure 7-1 Load Composition for the Mechanical Load

7.3.3 TRANSIENTS

The CSS is subjected to the thermal transients that are described in the CSS ASME Design Specification (Reference 4). For the CSS stress analysis, the enveloped transients described in CSS ASME Design Specification (Reference 4) are applied. They are the simplified multi-linear transients which produce more conservative thermal stresses because of combining the cycles of several RCS transients with less severe conditions than the enveloped transients. The RCS transients are described in the General ASME Design Specification (Reference 5). Some RCS design transients, such as the Reactor Coolant Pump startup and shutdown, are not included into the enveloped transients because the RCS temperature transients produce negligible fatigue usage in the CSS. The group name of each enveloped transient and the number of cycles are listed in Table 7-22 with the RCS transients. Table 7-23 shows the design transients for Level C and Level D Service. The mechanical loads associated with these transients are shown in Section 7.3.2.

Table 7-22 (1/2) Enveloped Transients at Level A and Level B Service

Group (Number of Cycles)	Mark	RCS Transient	Occurrence	Initial Temperature [°F]	
				Outlet	Inlet

Table 7-22 (2/2) Enveloped Transients at Level A and Level B Service

Group (Number of Cycles)	Mark	RCS Transient	Occurrence	Initial Temperature [°F]	
				Outlet	Inlet

Table 7-23 Design Transients at Level C and Level D Service

Level C

Mark	RCS Transient	Occurrence
III-a	Small loss of coolant accident	5
III-b	Small steam line break	5
III-c	Complete loss of flow	5
III-d	Small feed water line break	5
III-e	SG tube rupture	5

Level D

Mark	RCS Transient	Occurrence
IV-a	Large loss of coolant accident	1
IV-b	Large steam line break	1
IV-c	RCP locked rotor	1
IV-d	Control rod ejection	1
IV-e	Large feed water line break	1

7.3.4 HEAT GENERATION RATE

The internal heat generation was input to the structures surrounding the core, i.e. the lower CB, the LCSP, and the UCP. The average heat generation rates for each location are given in Table 7-24. Each rate was multiplied by the radial, circumferential and axial distribution factors from the CSS ASME Design Specification (Reference 4) to provide the distribution of the local three-dimensional heat generation rate in the component. The internal heating was combined with the thermal transients to determine the resulting metal temperatures for the thermal stress analysis.

Table 7-24 Average Heat Generation Rate

Location	Btu/ft^3/hr
LCSP	
Center Core Region	
Peripheral Core Region	
Out of Core Region	
CB	
UCP	
Center Core Region	
Peripheral Core Region	
Out of Core Region	

7.3.5 PRELOAD OF TSF

The extension and the bottom fastener of the USC and TSC are the TSF. The preload used for the stress evaluation are shown in Table 7-25.

Table 7-25 Preload of TSF

Parts	lbf
USC Bottom Fastener	
USC Extension	
TSC Bottom Fastener	
TSC Extension	

7.3.6 LOAD COMBINATIONS

The loading conditions consist of various combinations of the mechanical, thermal and external loads. The load combinations considered in the analysis are listed in Table 7-26.

Table 7-26 Load Combinations

System Operating Condition	Service Stress Limit	Service Loading Combination
Design	Design	· Static Mechanical Loads design pressure difference dead weight cross flow load interface load · Dynamic Mechanical Loads vibratory load
Normal / Upset	Level A & B	· Static Mechanical Loads pressure difference dead weight cross flow load interface load · Dynamic Mechanical Loads vibratory load 1/3 SSE load[1)] · Thermal loads enveloped transients internal heating · Preload[2)]
Emergency	Level C	· Static Mechanical Loads pressure difference dead weight cross flow load interface load · Dynamic Mechanical Loads vibratory load
Faulted	Level D	· Static Mechanical Loads pressure difference dead weight cross flow load interface load · Dynamic Mechanical Loads vibratory load SRSS(SSE + LOCA) Load

1) To consider in the fatigue analysis only
2) To consider only for the TSF

8.0 METHODOLOGY

The ABAQUS computer program (Reference 9) was used to calculate temperature distributions and stresses. ABAQUS is a general purpose finite element computer program used by MHI in the design and analysis of nuclear components. ABAQUS is available in the public domain and has been used by MHI for U.S. replacement Steam Generator and replacement Reactor Vessel closure head projects.

8.1 HEAT TRANSFER COEFFICIENT AND THERMAL ANALYSIS

The heat transfer coefficients on the inner and outer surfaces of the component are required to define the temperature distributions during transients. Classical Handbook heat transfer equations (References 10 and 11) were used to calculate the heat transfer coefficients, and the thermal properties in Section II, Part D of the ASME Code (Reference 3) were used in the determination of metal temperatures.

The finite element thermal analysis was performed for the CSS temperature transients to define the time-dependent temperature distributions of the structure. The primary coolant temperature versus time curve was applied to the wetted surfaces with the appropriate heat transfer coefficients. The heat generation rate was also input to the elements of the analysis models. MHI in-house proprietary computer program RIGHT was used to create the heat generation input data in the finite element analysis (FEA).

8.2 STRESS ANALYSIS

The stress analyses were performed using the FEA approach, which generates the stresses for the given loads and boundary conditions on the finite element model of the structure. The details of the model of each structural analysis are described in Section 10. The thermal loads were read from the thermal solution into each node of the structural model. The stresses were also derived by the hand calculations for the externally applied forces and moments.

For post processing the stresses in accordance with Subarticle NG-3200 of the ASME Code (Reference 1), the calculation of the stress intensities, stress classifications and stress evaluations were performed using a set of MHI in-house proprietary computer programs. These programs are CLASS3D, CLASS3DX, EDITSTRS, EVALPRI, EVALSEFAV, and RATCHET, which are summarized in Table 9-1.

The flowchart of the stress analysis and evaluation among these in-house computer programs is shown in Figure 8-1. CLASS3D and CLASS3DX classify the stresses resulting from the mechanical and thermal loads. EDITSTRS creates the input files for the stress evaluation programs, EVALPRI, EVALSEFAV, and RATCHET. These three programs were used for the evaluation of the primary stress, primary plus secondary stress, fatigue usage factors, and thermal ratchet.

For the TSF, stress analyses and evaluations were conducted by MHI in-house proprietary computer program SABRINA and the flowchart is shown in Figure 8-2.

8.3 FATIGUE ANALYSIS

The fatigue analysis was based on the rules of the ASME Code Section III (Reference 1). These rules require calculation of the total stress, including the peak stress, to determine the allowable number of the stress cycles for the specified Service Loadings at every point in the structure. In some cases, a fatigue strength reduction factor (FSRF) was used where the peak stress cannot be accurately calculated. The value of the FSRF was set at [ ]for the CSS and at [ ]for the TSF to consider conservatively.

The CSS enveloped thermal design transients described in Table 7-22 were used in the evaluation of fatigue caused by cyclic loading. The effect of 300 cycles of a 1/3 SSE seismic event was also included in the evaluation of fatigue, and treated as a Level B Service Condition. The number of cycles was based on the equivalent fatigue usage for a single SSE event of 20 cycles.

Figure 8-1 Flowchart of Stress Analysis and Evaluation for the CSS

Figure 8-2 Flowchart of Stress Analysis and Evaluation for TSF

9.0 COMPUTER PROGRAMS USED

Table 9-1 below provides a brief description of each of the computer programs used in the analyses. Refer to Figure 8-1 and Figure 8-2 for a visual description of the stress evaluation process. All these computer programs were verified and validated in compliance with MHI quality assurance program. The computer programs were validated using one of the methods described below. Verification tests demonstrate the capability of the computer program to produce valid results for the test problems encompassing the range of permitted usage defined by the program documentation.

Computer program validation methods include:

· Hand calculations

· Known solution for similar or standard problem

· Acceptable experimental test results

· Published analytical results

· Results from other similar verified program

Table 9-1 Summary of Computer Programs Used

No.	Program Name	Version	Description
1	ABAQUS	6.7-1	ABAQUS is a finite element computer code, which enables a wide range of linear and nonlinear engineering simulations
2	RIGHT	0.0	RIGHT is an MHI Code to create the internal heating files of 3D solid Models
3	CLASS3D	3.0	CLASS3D is an MHI Code to classify the stress on line for 3D solid Models.
4	CLASS3DX	0.0	CLASS3DX is an MHI Code to classify the stress on plane for 3D solid Models.
5	EDITSTRS	3.0	EDITSTRS is an MHI Code to create input files for the stress evaluation program.
6	EVALPRI	5.0	EVALPRI is an MHI code to perform the primary stress evaluation.
7	EVALSEFAV	4.0	EVALSEFAV is an MHI code to perform secondary stress and fatigue evaluation.
8	RATCHET	5.0	RATCHET is an MHI code to evaluate thermal ratcheting.
9	ASMETEMP	0.0	ASMETEMP is an MHI Code to create temperature files for stress evaluation program.
10	SABRINA	0.0	SABRINA is an MHI Code to perform the stress evaluation for the TSF.

10.0 STRUCTURAL ANALYSIS RESULTS

The stress calculations were completed using a combination of the FEA and hand calculations.

The general element type used for creation of the finite element model was a 20-node quadratic brick from the ABAQUS element library for the heat transfer and structural analysis. The following three models are generated for the Thermal and stress analyses;

(1) The Lower CSS model that contains the CB and LCSP,

(2) The Upper CSS model that contains the UCS, UCP, USC and TSC,

(3) The RSK model.

In these models, many through-thickness lines and planes that would be subjected to a large stress were selected and defined as Stress Classification Lines (SCL) and Stress Classification Planes (SCP). The stress evaluations were performed on the SCL and SCP.

The calculated results were conservative compared to the values that would be determined if more detailed calculations were performed. However, since the ASME Code allowable limits were satisfied in all cases, further analysis was not necessary.

10.1 LOWER CSS

10.1.1 MODELING AND ANALYSIS

The dimensions of the lower CSS are shown in Figure 10-1. For the stress analyses of the CB and the LCSP, the three-dimensional finite element model of the 45° sector of the lower CSS was developed considering the symmetrical properties of the structures and the load configurations. Figure 10-2 shows the three-dimensional finite element model. The SCL or SCP was selected on the structural discontinuities and the ligaments between holes. The outlet nozzles in the upper CB were not modeled because they are not CSS and do not affect the structural integrity of the CB in the selected areas; however, the dead weight of the nozzles was taken into account in the upper CB to adjust its mass density. The mesh divisions are presented in detail in Figure 10-3 and Figure 10-4.

To simulate the structural behavior of the lower CSS, the vertical displacement of the CB flange lower surface at the support ledge of the Reactor Vessel was fixed.

The finite element thermal analyses were performed for Level A and Level B Service Conditions. The Outlet temperature was used as the thermal boundary conditions for the inner surface of the upper CB. The Inlet temperature was used for the rest.

The stress calculations were based on the loading conditions shown in Section 7.3.

Figure 10-1 (1/2) Lower CSS Dimensions

Figure 10-1 (2/2) Lower CSS Dimensions

Figure 10-2 General Aspect of the Lower CSS FEA Model

Figure 10-3 FEA Model of the Upper CB / Flange Discontinuity

Figure 10-4 FEA Model of the LCSP and the Lower CB / LCSP Discontinuity

10.1.2 STRESS RESULTS

Figures 10-5 through 10-8 show the SCL and SCP for the lower CSS. The calculated stress-to-allowable ratio (calculated stress divided by allowable value) and the cumulative fatigue usage factor for the most limiting locations are summarized in Tables 10-1 through 10-8. The highest cumulative fatigue usage factor for the CB occurred at the SCL-39 in Figure 10-6. The factor for the LCSP occurred at the SCP-02 in Figure 10-8.

Table 10-1 CB - Primary Stress Result Summary

Evaluation Part	Condition	P_m Stress to Allowable Ratio	P_m+P_b Stress to Allowable Ratio
CB Flange / Upper CB discontinuity	Design		
	Level A / Level B		
	Level C		
	Level D		
Upper CB / Lower CB discontinuity	Design		
	Level A / Level B		
	Level C		
	Level D		
Lower CB / LCSP discontinuity	Design		
	Level A / Level B		
	Level C		
	Level D		

Table 10-2 LCSP - Primary Stress Result Summary

Evaluation Part	Condition	P_m Stress to Allowable Ratio	P_m+P_b Stress to Allowable Ratio
Ligament between core inlet flow holes	Design		
	Level A / Level B		
	Level C		
	Level D		

Table 10-3 CB - Primary Plus Secondary Stress Result Summary

Evaluation Part	Condition	P_m+P_b+Q Stress to Allowable Ratio	Fatigue Cumulative Usage Factor, ΣU
CB Flange / Upper CB discontinuity	Level A / Level B		
Upper CB / Lower CB discontinuity	Level A / Level B		
Lower CB / LCSP discontinuity	Level A / Level B		

Table 10-4 LCSP - Primary Plus Secondary Stress Result Summary

Evaluation Part	Condition	P_m+P_b+Q Stress to Allowable Ratio	Fatigue Cumulative Usage Factor, ΣU
Ligament between core inlet flow holes	Level A / Level B		

Table 10-5 CB - Triaxial Stress Result Summary

Evaluation Part	Condition	Triaxial Stress Stress to Allowable Ratio
CB Flange / Upper CB discontinuity	Design	
	Level A / Level B	
	Level C	
	Level D	
Upper CB / Lower CB discontinuity	Design	
	Level A / Level B	
	Level C	
	Level D	
Lower CB / LCSP discontinuity	Design	
	Level A / Level B	
	Level C	
	Level D	

Table 10-6 LCSP - Triaxial Stress Result Summary

Evaluation Part	Condition	Triaxial Stress Stress to Allowable Ratio
Ligament between core inlet flow holes	Design	
	Level A / Level B	
	Level C	
	Level D	

Table 10-7 CB - Bearing Stress Result Summary

Evaluation Part	Condition	Bearing Stress Stress to Allowable Ratio
CB Flange lower surface to RV support ledge	Design	
	Level A / Level B	
	Level C	
	Level D	
CB Flange outer to RV inner Surface	Design	
	Level A / Level B	
	Level C	
	Level D	

Table 10-8 CB – External Pressure Result Summary

Evaluation Part	External Pressure Pressure to Allowable Ratio
CB	

Figure 10-5 SCL for CB Flange / Upper CB Discontinuity

Figure 10-6 SCL for Upper / Lower CB Discontinuity

Figure 10-7 SCL for Lower CB / LCSP Discontinuity

Figure 10-8 SCP for LCSP Ligaments between Core Inlet Flow Holes

10.2 UPPER CSS

10.2.1 MODELING AND ANALYSIS

The dimensions of the upper CSS are shown in Figure 10-9. For the stress analyses of the UCS, UCP, USC and TSC, the three-dimensional finite element model of the 90° sector of the upper CSS was developed considering the symmetrical properties of the structures and the load configurations. Figure 10-10 shows the three-dimensional finite element model. The SCL or SCP was selected on the structural discontinuities and the ligaments between holes. The mesh divisions are presented in detail in Figures 10-11 through 10-13.

To simulate the structural behavior of the upper CSS, the vertical movement on the interface between the UCS flange upper surface and the closure head of the Reactor Vessel was fixed.

The finite element thermal analyses were performed for Level A and Level B Service Conditions. The Outlet temperature was used as the thermal boundary condition for all surfaces in the upper plenum and the bottom surface of the UCP in the core region. The Inlet temperature was used for the rest.

The stress calculations were based on the loading conditions shown in Section 7.3.

Figure 10-9 (1/4) Upper CSS Dimensions

Figure 10-9 (2/4) Upper CSS Dimensions

Figure 10-9 (3/4) Upper CSS Dimensions

Figure 10-9 (4/4) Upper CSS Dimensions

Figure 10-10 General Aspect of the Upper CSS FEA Model

Figure 10-11 FEA Model of the UCS

Figure 10-12 FEA Model of the UCP

Figure 10-13 FEA Model of the USC and the TSC

10.2.2 STRESS RESULTS

Figures 10-14 through 10-20 show the SCL and SCP for the upper CSS. The calculated stress-to-allowable ratio (calculated stress divided by allowable value) and the cumulative fatigue usage factor for the most limiting locations are summarized in Tables 10-9 through 10-19 for the upper CSS. Since the primary plus secondary stress range only for UCS Flange/Skirt discontinuity exceeded $3S_m$, the thermal ratchet evaluation was performed and its stress-to-allowable ratio was〔 〕, which was acceptable. The highest cumulative fatigue usage factor for the UCS occurred at the SCP-01 in Figure 10-16. The factor for the UCP occurred at SCP-11 in Figure 10-17. The factor for the USC occurred at the SCL-532 in Figure 10-20.

Table 10-9 UCS - Primary Stress Result Summary

Evaluation Part	Condition	P_m Stress to Allowable Ratio	P_m+P_b Stress to Allowable Ratio
Flange / Skirt discontinuity	Design		
	Level A / Level B		
	Level C		
	Level D		
Skirt / Plate discontinuity	Design		
	Level A / Level B		
	Level C		
	Level D		
Ligament between Plate Holes	Design		
	Level A / Level B		
	Level C		
	Level D		

Table 10-10 UCP - Primary Stress Result Summary

Evaluation Part	Condition	P_m Stress to Allowable Ratio	P_m+P_b Stress to Allowable Ratio
Ligament between Core Oultlet Flow Holes	Design		
	Level A / Level B		
	Level C		
	Level D		

Table 10-11 USC - Primary Stress Result Summary

Evaluation Part	Condition	P_m Stress to Allowable Ratio	P_m+P_b Stress to Allowable Ratio
USC Body	Design		
	Level A / Level B		
	Level C		
	Level D		
TSC Body	Design		
	Level A / Level B		
	Level C		
	Level D		

Table 10-12 UCS - Primary Plus Secondary Stress Result Summary

Evaluation Part	Condition	P_m+P_b +Q Stress to Allowable Ratio	Fatigue Cumulative Usage Factor, ΣU
Flange / Skirt discontinuity	Level A / Level B		
Skirt / Plate discontinuity	Level A / Level B		
Ligament between Plate Holes	Level A / Level B		

Table 10-13 UCP - Primary Plus Secondary Stress Result Summary

Evaluation Part	Condition	P_m+P_b +Q Stress to Allowable Ratio	Fatigue Cumulative Usage Factor, ΣU
Ligament between Core Oultlet Flow Holes	Level A / Level B		

Table 10-14 USC - Primary Plus Secondary Stress Result Summary

Evaluation Part	Condition	P_m+P_b +Q Stress to Allowable Ratio	Fatigue Cumulative Usage Factor, ΣU
USC Body	Level A / Level B		
TSC Body	Level A / Level B		

Table 10-15 UCS –Triaxial Stress Result Summary

Evaluation Part	Condition	Triaxial Stress Stress to Allowable Ratio
Flange / Skirt discontinuity	Design	
	Level A / Level B	
	Level C	
	Level D	
Skirt / Plate discontinuity	Design	
	Level A / Level B	
	Level C	
	Level D	
Ligament between Plate Holes	Design	
	Level A / Level B	
	Level C	
	Level D	

Table 10-16 UCP - Triaxial Stress Result Summary

Evaluation Part	Condition	Triaxial Stress Stress to Allowable Ratio
Ligament between Core Oultlet Flow Holes	Design	
	Level A / Level B	
	Level C	
	Level D	

Table 10-17 USC -Triaxial Stress Result Summary

Evaluation Part	Condition	Triaxial Stress Stress to Allowable Ratio
USC Body	Design	
	Level A / Level B	
	Level C	
	Level D	
TSC Body	Design	
	Level A / Level B	
	Level C	
	Level D	

Table 10-18 UCS -Bearing Stress Result Summary

Evaluation Part	Condition	Bearing Stress Stress to Allowable Ratio
UCS Flange upper Surface to RV Closure Head	Design	
	Level A / Level B	
	Level C	
	Level D	

Table 10-19 USC and TSC – Compressive Stress Result Summary

Evaluation Part	Compressive Stress
	Stress to Allowable Ratio
USC Body	
TSC Body	

Figure 10-14 SCL for UCS Flange / Skirt Discontinuity

Figure 10-15 SCL for UCS Skirt / Plate Discontinuity

Figure 10-16 SCP for UCS Plate Ligaments between Holes

Figure 10-17 SCP for UCP Ligaments between Core Outlet Flow Holes

Figure 10-18 SCL for USC

Figure 10-19 SCL for TSC

Figure 10-20 SCL for USC and TSC

10.3 RSK

10.3.1 Modeling and Analysis

The dimensions of the RSK are shown in Figure 10-21. For the stress analyses of the RSK, the three-dimensional finite element model was developed as shown in Figure 10-22. The SCP was selected near the root of the key body.

To simulate the structural behavior of the RSK, the movement of the connection part to the LCSP was fixed.

The finite element thermal analyses were performed for Level A and Level B Service Conditions. The Inlet temperature was used as the thermal boundary condition for all surfaces of the RSK.

The stress calculations were based on the loading conditions shown in Section 7.3.

Figure 10-21 RSK Dimensions

Figure 10-22 General Aspect of the RSK FEA Model

10.3.2 STRESS RESULTS

Figure 10-23 shows the SCP for the RSK. The calculated stress-to-allowable ratio (calculated stress divided by allowable value) and the cumulative fatigue usage factor are summarized in Tables 10-20 through 10-23. The highest cumulative fatigue usage factor for the RSK occurred at the SCP-05 in Figure 10-23.

Table 10-20 RSK - Primary Stress Result Summary

Evaluation Part	Condition	P_m Stress to Allowable Ratio	P_m+P_b Stress to Allowable Ratio
Key Body	Design		
	Level A / Level B		
	Level C		
	Level D		

Table 10-21 RSK - Primary Plus Secondary Stress Result Summary

Evaluation Part	Condition	P_m+P_b+Q Stress to Allowable Ratio	Fatigue Cumulative Usage Factor, ΣU
Key Body	Level A / Level B		

Table 10-22 RSK - Triaxial Stress Result Summary

Evaluation Part	Condition	Triaxial Stress Stress to Allowable Ratio
Key Body	Design	
	Level A / Level B	
	Level C	
	Level D	

Table 10-23 RSK – Bearing Stress Result Summary

Evaluation Part	Condition	Bearing Stress Stress to Allowable Ratio
Key Body	Design	
	Level A / Level B	
	Level C	
	Level D	

Figure 10-23 SCP for RSK

10.4 TSF

10.4.1 Modeling and Analysis

The stress analysis and evaluation for the TSF were performed by the method described in Section 8.

10.4.2 Stress Results

The calculated stress-to-allowable ratio (calculated stress divided by allowable value), and the cumulative fatigue usage factor are summarized in Tables 10-24 through 10-27. The highest cumulative fatigue usage factor for the TSF occurred at the USC Extension.

Table 10-24 TSF - Primary Stress Result Summary

Evaluation Part	Condition	P_m Stress to Allowable Ratio	P_m+P_b Stress to Allowable Ratio
USC Extension	Design		
	Level A / Level B		
	Level C		
	Level D		
TSC Extension	Design		
	Level A / Level B		
	Level C		
	Level D		
USC Bottom Fastener	Design		
	Level A / Level B		
	Level C		
	Level D		
TSC Bottom Fastener	Design		
	Level A / Level B		
	Level C		
	Level D		

Table 10-25 TSF - Primary Plus Secondary Stress Result Summary

Evaluation Part	Condition	P_m+Q_m Stress to Allowable Ratio	$P_m+P_b+Q_m+Q_b$ Stress to Allowable Ratio	Fatigue Cumulative Usage Factor, ΣU
USC Extension	Level A / Level B			
TSC Extension	Level A / Level B			
USC Bottom Fastener	Level A / Level B			
TSC Bottom Fastener	Level A / Level B			

Table 10-26 TSF - Average Bearing Stresses Result Summary

Evaluation Part	Condition	Bearing Stress Stress to Allowable Ratio
USC Extension	Level A / Level B	
TSC Extension	Level A / Level B	
USC Bottom Fastener	Level A / Level B	
TSC Bottom Fastener	Level A / Level B	

Table 10-27 TSF – Membrane Stresses during Installation Summary

Evaluation Part	Condition	Membrane Stress for Torquing Stress to Allowable Ratio
USC Extension	Level A / Level B	
TSC Extension	Level A / Level B	
USC Bottom Fastener	Level A / Level B	
TSC Bottom Fastener	Level A / Level B	

11.0 REFERENCES

1. ASME Boiler and Pressure Vessel Code, Section III Division 1, 2001 Edition with 2003 Addenda

2. ASME Boiler and Pressure Vessel Code, Section III Appendix F, 2001 Edition with 2003 Addenda

3. ASME Boiler and Pressure Vessel Code, Section II Part D, 2001 Edition with 2003 Addenda

4. N0-EC40001 Revision 1 "US-APWR Standard Design Core Support Structures ASME Design Specification"

5. N0-FB10L01 Revision 0 "US-APWR Standard Design General ASME Design Specification for Class 1 and CS Components

6. (MHI's commitment letter) Additional Information for Design Completion Plan of US-APWR Piping and Components" UAP-HF-08123, July, 2008.

7. N0-EC40101 Revision 0 "Core Support Structures Design Drawings"

8. Case N-60-5 – Material for Core Support Structures Section III, Division 1

9. SIMULIA, "ABAQUS Analysis User's Manual", Version 6.7, 2007

10. Warren M. Rohsenow, James P. Hartnett and Young I. Cho, "Handbook of Heat Transfer", Third Edition, McGraw Hill, 1998

11. JSME Data Book : Heat Transfer (4th Edition)